Simulation of MgO/AA6061 Particulate-Reinforced Composites Taking Account of CTE Mismatch Effects and Interphase Separation

A. Chennakesava Reddy

Associate Professor, Department of Mechanical Engineering, Vasavi College of Engineering, Hyderabad, India
dr_acreddy@yahoo.com

Abstract: In the present work, the MgO/AA6061 alloy metal matrix composites were subjected to mechanical and thermal loads. The results obtained from the finite element analysis of MgO/AA6061 alloy composites reveal the interphase separation from the particle and the matrix. No particle fracture has been noticed in MgO/AA6061 composites.

Keywords: Magnesium oxide, AA6061 alloy, RVE model, finite element analysis, interphase separation.

1. INTRODUCTION

A major failure mode in composites is debonding, either between matrix and reinforcement. Debonding of particle/matrix interfaces in composites may significantly affect their macroscopic behavior since interface debonding leads to crack initiation and propagation. The unit cell methods can easily account for complex microstructural morphology and can enable the investigation of the influence of different geometrical features on the overall response. There are at least two interface properties that can influence the results. First, the interface plays a role in the ability of the matrix to transfer stress back into the broken particle in the metal matrix composites. Stress transfer needs to occur before more particle fractures take place. Second, the interface itself may fail. Stress transfer and interfacial failure are distinct properties of the interface. Finite element analysis for a unit cell containing one particle in a matrix was widely applied to fracture or debonding of particles [1]. In a series of research works carried out recently, the interface debonding was studied in composites subject to uniaxial tension since it is a widely used test to characterize the material behavior [2-15].

The aim of the present work is predict the influence of volume fraction and the mismatch of thermal expansion in magnesium oxide/AA6061 alloy composites on interphase separation and particle fracture. The shape magnesium oxide particle is spherical. The periodic particle distribution was a square array and corresponding representative volume element (RVE) is showed in figure 1.

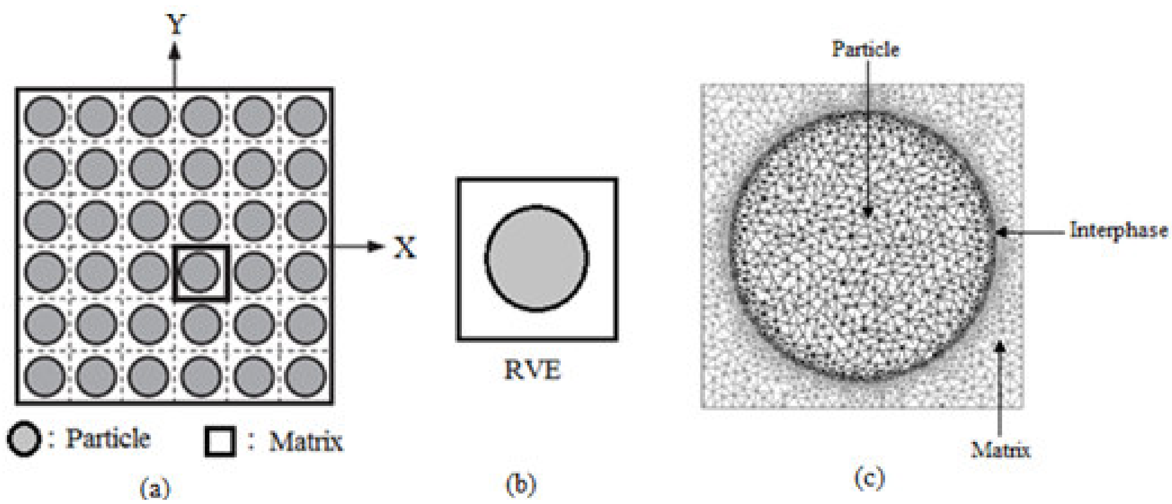

Figure 1: Square array of particles (a); Representative Volume Element (b); and Discretization of RVE (c).

2. MATERIALS METHODS

The matrix material was AA6061 alloy. The reinforcement material was magnesium oxide (MgO) nanoparticles of average size 100nm. The mechanical properties of materials used in the present work are given in table 1. In the current work, a cubical representative volume element (RVE) was implemented to analyze the tensile behavior MgO/AA6061 alloy composites at two (10% and 30%) volume fractions of MgO and at different temperatures. The large strain PLANE183 element was used in the matrix in all the models. In order to model the adhesion between the matrix and the particle, a CONTACT 172 element was used.

Table 1: Mechanical properties of AA6061 matrix and MgO nanoparticles

Property	AA6061	MgO
Density, g/cc	2.70	3.54
Elastic modulus, GPa	68.9	270.0
Coefficient of thermal expansion, 10^{-6} 1/°C	23.6	12.0
Specific heat capacity, J/kg/°C	896	1030
Thermal conductivity, W/m/°C	167	60
Poisson's ratio	0.33	0.35

3. RESULTS AND DISCUSSION

The elastic moduli are normalized with the elastic modulus (E_m) of AA6061 alloy. The normalized elastic moduli, E_x/E_m and E_y/E_m, are decreased with increase of thermal loading (figure 2a). E_x/E_m is higher than E_y/E_m due to tensile loading along x-direction. The normalized shear modulus increases with increase of temperature as shown in figure 2b. The increase of major Poisson's ratio with increase of temperature from 100°C to 300°C indicates the elongation along the load is greater than that along the transverse direction of loading of RVE (figure 2c). The decrease of Poison's ratio from 30°C to 100°C is not clear.

If the particle deforms in an elastic manner (according to Hooke's law) then,

$$\tau = \frac{n}{2}\sigma_p \quad (1)$$

where σ_p is the particle stress. For the interfacial debonding/yielding to occur, the interfacial shear stress reaches its shear strength:

$$\tau = \tau_{max} \quad (2)$$

For particle/matrix interfacial debonding can occur if the following condition is satisfied:

$$\tau_{max} < \frac{n\sigma_p}{2} \quad (3)$$

The interphase separation occurs between MgO nanoparticle and AA6061 alloy matrix as seen from figure 3 as the condition in Eq.(3) is satisfied. If particle fracture occurs when the stress in the particle reaches its ultimate tensile strength, $\sigma_{p,uts}$, then setting the boundary condition at

$$\sigma_p = \sigma_{p,\,uts} \quad (4)$$

The relationship between the strength of the particle and the interfacial shear stress is such that if

$$\sigma_{P,uts} < \frac{2\tau}{n} \quad (5)$$

Then the particle will fracture. From the figure 3b, it is observed that the MgO nanoparticle is not as the condition in Eq. (5) is not satisfied.

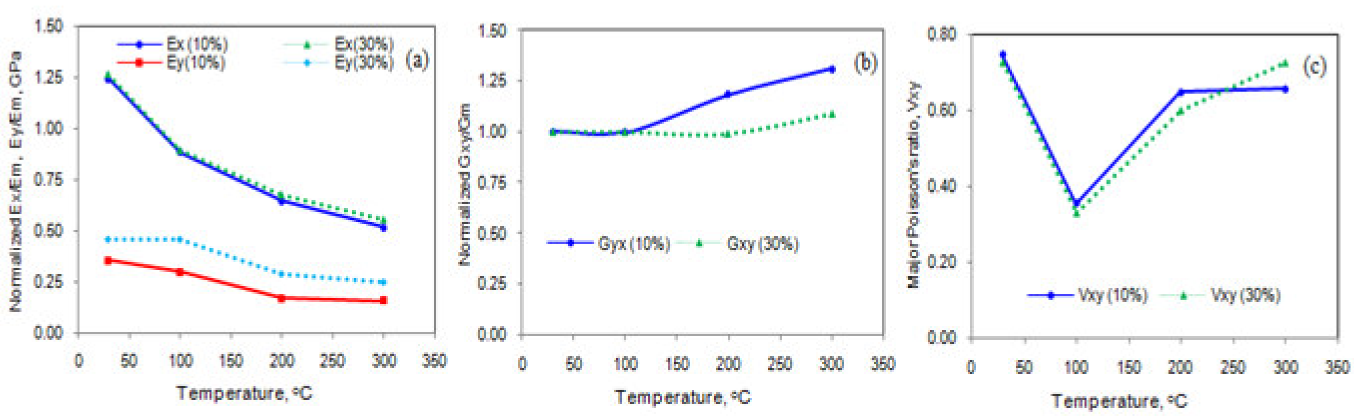

Figure 2: Effect of temperature on micromechanical properties of MgO/AA6061 composites.

The von Mises stress as a function of temperature is illustrated in figure 4. The von Mises stresses induced at the interface are higher than that induced in the nanoparticle. Hence, the interphase separation has occurred between the particle and the matrix.

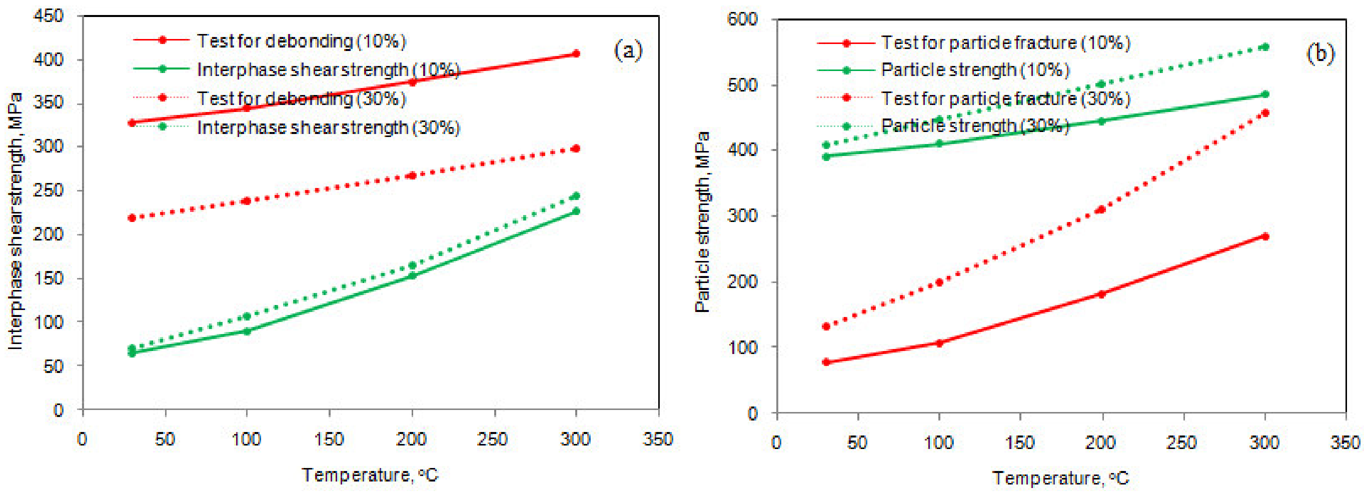

Figure 3: Criterion for interfacial debonding (a) and for particle fracture (b).

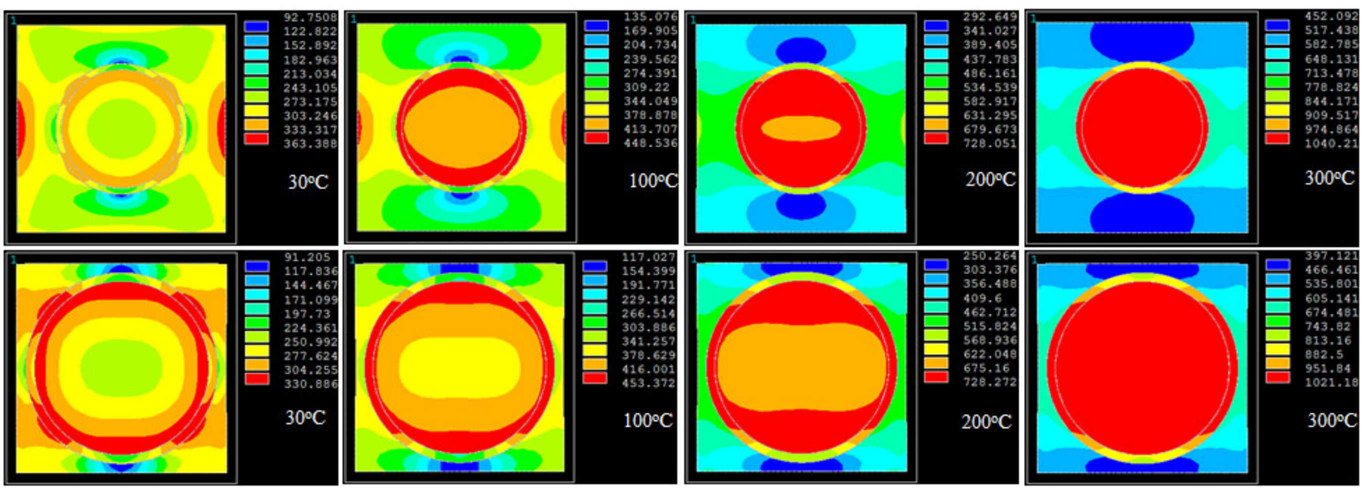

Figure 4: Images of von Mises stresses obtained from FEA: (a) 10% MgO/AA6061 alloy and (b) 30% MgO/AA6061 alloy composites.

4. CONCLUSION

The shear stress is high at the interface resulting to interphase separation from the particle and the matrix. The interphase separation has occurred between the particle and the matrix in MgO/AA6061 composites. The fracture of MgO particle was not observed.

REFERENCES

1. J. R. Brockenbrough, F. W. Zok, On the role of Particle Cracking in Flow and Fracture of Metal Matrix Composites. Acta Metallurgica & Materialia, 43, 1995, pp.11-20.
2. A. Chennakesava Reddy, Evaluation of Debonding and Dislocation Occurrences in Rhombus Silicon Nitride Particulate/AA4015 Alloy Metal Matrix Composites, 1st National Conference on Modern Materials and Manufacturing, Pune, India, 19-20 December 1997, pp. 278-282.
3. A. Chennakesava Reddy, Interfacial Debonding Analysis in Terms of Interfacial Tractions for Titanium Boride/AA3003 Alloy Metal Matrix Composites, 1st National Conference on Modern Materials and Manufacturing , Pune, 19-20 December, 1997.
4. A. Chennakesava Reddy, Assessment of Debonding and Particulate Fracture Occurrences in Circular Silicon Nitride Particulate/AA5050 Alloy Metal Matrix Composites , National Conference on Materials and Manufacturing Processes, Hyderabad, India, 27-28 February 1998, pp. 104-109.
5. A. Chennakesava Reddy, Local Stress Differential for Particulate Fracture in AA2024/Titanium Carbide Nanoparticulate Metal Matrix Composites, National Conference on Materials and Manufacturing Processes, Hyderabad, India, 27-28 February 1998, pp. 127-131.
6. A. Chennakesava Reddy, Micromechanical Modelling of Interfacial Debonding in AA1100/Graphite Nanoparticulate Reinforced Metal Matrix Composites, 2nd International Conference on Composite Materials and Characterization, Nagpur, India, 9-10 April 1999, pp. 249-253.

7. A. Chennakesava Reddy, Cohesive Zone Finite Element Analysis to Envisage Interface Debonding in AA7020/Titanium Oxide Nanoparticulate Metal Matrix Composites, 2nd International Conference on Composite Materials and Characterization, Nagpur, India, 9-10 April 1999, pp. 204-209.
8. H. B. Niranjan, A. Chennakesava Reddy, Computational Modeling of Interfacial Debonding in Fused Silica/AA7020 Alloy Particle-Reinforced Metal Matrix Composites, 3rd International Conference on Composite Materials and Characterization, Chennai, India, 11-12 May 2001, pp. 222-227.
9. H. B. Niranjan, A. Chennakesava Reddy, Nanoscale Characterization of Interfacial Debonding and Matrix Damage in Titanium Carbide/AA8090 Alloy Particle-Reinforced Metal Matrix Composites, 3rd International Conference on Composite Materials and Characterization, Chennai, India, 11-12 May 2001, pp. 228-233.
10. S. Sundara Rajan, A. Chennakesava Reddy, Assessment of Temperature Induced Fracture in Boron Nitride/AA1100 Alloy Particle-Reinforced Metal Matrix Composites, 3rd International Conference on Composite Materials and Characterization, Chennai, India, 11-12 May 2001, pp. 234-239.
11. S. Sundara Rajan, A. Chennakesava Reddy, Estimation of Fracture in Zirconia/AA2024 Alloy Particle-Reinforced Composites Subjected to Thermo-Mechanical Loading, 3rd International Conference on Composite Materials and Characterization, Chennai, India, 11-12 May 2001, pp. 240-245.
12. P. M. Jebaraj, A. Chennakesava Reddy, Finite Element Predictions for the Thermoelastic Properties and Interphase Fracture of Titanium Nitride /AA3003 Alloy Particle-Reinforced Composites, 3rd International Conference on Composite Materials and Characterization, Chennai, India, 11-12 May 2001, pp. 246-251.
13. P. M. Jebaraj, A. Chennakesava Reddy, Effect of Thermo-Mechanical Loading on Interphase and Particle Fractures of Titanium Oxide /AA4015 Alloy Particle-Reinforced Composites, 3rd International Conference on Composite Materials and Characterization, Chennai, India, 11-12 May 2001, pp. 252-256.
14. A. Chennakesava Reddy, Effect of CTE and Stiffness Mismatches on Interphase and Particle Fractures of Zirconium Carbide /AA5050 Alloy Particle-Reinforced Composites, 3rd International Conference on Composite Materials and Characterization, Chennai, India, 11-12 May 2001, pp. 257-262.
15. A. Chennakesava Reddy, Behavioral Characteristics of Graphite /AA6061 Alloy Particle-Reinforced Metal Matrix Composites, 3rd International Conference on Composite Materials and Characterization, Chennai, India, 11-12 May 2001, pp. 263-269.